Contribution from the Department of Chemistry, Faculty of Science, Tohoku University, Aoba, Aramaki, Aoba-ku, Sendai 980, Japan

Kinetic Studies on the Terminal-Ligand-Substitution Reactions of Acetate-Bridged Trinuclear Molybdenum and Tungsten Cluster Complexes, $[Mo_3(\mu_3\text{-}CCH_3)(\mu_3\text{-}O)(\mu\text{-}CH_3COO)_6(L)_3]^+$ (L = H_2O or Pyridine) and $[W_3(\mu_3\text{-}O)(\mu\text{-}CH_3COO)_6(H_2O)_3]^{2+}$

Kou Nakata, Akira Nagasawa,[1] Nobuyuki Soyama, Yoichi Sasaki,* and Tasuku Ito*

Received June 29, 1990

Three different reactions of trinuclear acetato-bridged molybdenum and tungsten cluster complexes have been studied by following the change in ^1H NMR spectra. Stepwise substitution reactions of solvent CD_3OD for the terminal aqua ligands on $[Mo_3(\mu_3\text{-}CCH_3)(\mu_3\text{-}O)(\mu\text{-}CH_3COO)_6(H_2O)_3]^+$ (formal oxidation state of the Mo_3 is (IV,IV,IV)) (−30.2 to −15.3 °C) and $[W_3(\mu_3\text{-}O)(\mu\text{-}CH_3COO)_6(H_2O)_3]^{2+}$ (III,III,IV) (9.5–29.6 °C) in CD_3OD gave first-order rate constants (per metal ion) of the first steps of $(9.4 \pm 1.5) \times 10^{-5}$ s^{-1} at −22.5 °C ($\Delta H^* = 93 \pm 11$ kJ mol^{-1}; $\Delta S^* = +49 \pm 47$ J K^{-1} mol^{-1}) and $(5.5 \bullet 0.6) \times 10^{-5}$ s^{-1} at 24.5 °C ($\Delta H^* = 113 \pm 3$ kJ mol^{-1}; $\Delta S^* = +56 \bullet 9$ J K^{-1} mol^{-1}), respectively. A pyridine exchange reaction with py-d_5 (0.5–2.6 M) for the new complex $[Mo_3(\mu_3\text{-}CCH_3)(\mu_3\text{-}O)(\mu\text{-}CH_3COO)_6(py)_3]^+$ in CD_3NO_2 shows no [py-d_5] dependence at 10–35 °C. The first-order rate constant at 20.8 °C is $(8.6 \pm 1.0) \times 10^{-4}$ s^{-1} ($\Delta H^* = 112 \pm 1$ kJ mol^{-1}; $\Delta S^* = +77 \pm 5$ J K^{-1} mol^{-1}) (−0.3 to +34.6 °C). Results for the two $Mo_3(\mu_3\text{-}CCH_3)(\mu_3\text{-}O)$ complexes clearly indicate a strong dependence of the substitution rates on the type of leaving ligands even if the difference in solvents is taken into account. The CD_3OD substitution rate constant is significantly larger than the corresponding value (1.1×10^{-5} s^{-1} at 44.8 °C per metal ion) for the bis(μ_3-oxo) complex $[Mo_3(\mu_3\text{-}O)_2(\mu\text{-}CH_3COO)_6(H_2O)_3]^{2+}$ (IV,IV,IV), indicating a strong labilization effect of the μ_3-CCH_3^{3-} ligand. The rate constant for the W_3 complex is at least 2×10^3 times larger than that ($< 5 \times 10^{-7}$ s^{-1} at 44.8 °C) for the double-capped complex $[W_3(\mu_3\text{-}O)_2(\mu\text{-}CH_3COO)_6(H_2O)_3]^{2+}$ (IV,IV,IV). A difference in the formal oxidation state should be responsible in this case. An I_d or D mechanism is suggested for all the terminal ligand substitution reactions of these trinuclear cluster compounds.

Introduction

Molybdenum and tungsten in the oxidation state around IV give a variety of trinuclear complexes with metal–metal direct bonds.[2,3] When carboxylate ions are the ligands, they give the complexes with a characteristic $(\mu_3\text{-oxo})_2(\mu\text{-RCOO})_6$ core structure, $[M^{IV}_3(\mu_3\text{-}O)_2(\mu\text{-RCOO})_6(A)_3]^{2+}$ (M = Mo, W; R = CH_3, C_2H_5, C_6H_5, etc.; A = H_2O, etc.) (Chart Ia).[3] Mixed molybdenum–tungsten complexes, $[Mo_nW_{3-n}(\mu_3\text{-}O)_2(\mu\text{-}CH_3COO)_6(H_2O)_3]^{2+}$ (n = 1, 2), have also been prepared,[4] which further demonstrate the easy accessibility to such structure. Analogous complexes with capping CCH_3^{3-} are known, $[M^{IV}_3(\mu_3\text{-}CCH_3)(\mu_3\text{-}O)(\mu\text{-}CH_3COO)_6(H_2O)_3]^+$ (M = Mo,[5–8] W[9]) (Chart Ib) and $[Mo_3(\mu_3\text{-}CCH_3)_2(\mu\text{-}CH_3COO)_6(H_2O)_3]^{n+}$ (oxidation state of the Mo_3 is (IV,IV,V) when n = 1 and (IV,V,V) when n = 2).[5,10] A tungsten complex with only one oxide cap, $[W_3(\mu_3\text{-}O)(\mu\text{-}CH_3COO)_6(H_2O)_3]^{2+}$, was reported (Chart Ic),[11,12] where the formal oxidation state of the W_3 is (III,III,IV). It is apparent that the stable oxidation state varies with the change in the capping groups.

We are interested in their ligand substitution properties with reference to the influence of the kind of metal ions, capping groups, and formal oxidation states, as well as that of the metal–metal bond. Rates of the terminal ligand substitution of the bis(μ_3-oxo)–Mo_3 and –W_3 complexes were measured for the following reactions in CD_3OD.[13]

$$[M_3(\mu_3\text{-}O)_2(\mu\text{-}CH_3COO)_6(H_2O)_3]^{2+} + CD_3OD \rightarrow [M_3(\mu_3\text{-}O)_2(\mu\text{-}CH_3COO)_6(H_2O)_2(CD_3OD)]^{2+} + H_2O \quad (1)$$

M = Mo or W

At 44.8 °C, the first-order rate constants are 1.1×10^{-5} and $< 5 \times 10^{-7}$ s^{-1} per metal ion for the Mo_3 and W_3 complexes, respectively.[13] Thus the Mo complex is at least 20 times more labile than the W complex.

In order to find out the influence of the capping groups, we have planned to study the terminal ligand substitution of the CCH_3-capped Mo_3 complexes by monitoring the ^1H NMR spectra. It turned out to be difficult to study this with the $Mo_3(\mu_3\text{-}CCH_3)_2$ complexes because they are paramagnetic and unstable for time-consuming measurements. In addition to the CD_3OD substitution in CD_3OD (eq 2), we have studied the pyridine exchange reaction (eq 3) by the use of a newly prepared pyridine (py)

$$[Mo_3(\mu_3\text{-}CCH_3)(\mu_3\text{-}O)(\mu\text{-}CH_3COO)_6(H_2O)_3]^+ + 3CD_3OD \rightarrow [Mo_3(\mu_3\text{-}CCH_3)(\mu_3\text{-}O)(\mu\text{-}CH_3COO)_6(CD_3OD)_3]^+ + 3H_2O \quad (2)$$

$$[Mo_3(\mu_3\text{-}CCH_3)(\mu_3\text{-}O)(\mu\text{-}CH_3COO)_6(py)_3]^+ + 3py\text{-}d_5 \rightarrow [Mo_3(\mu_3\text{-}CCH_3)(\mu_3\text{-}O)(\mu\text{-}CH_3COO)_6(py\text{-}d_5)_3]^+ + 3py \quad (3)$$

Chart I. Structures of the Complexes Relevant to This Work:
(a) $[M_3(\mu_3\text{-}O)_2(\mu\text{-}CH_3COO)_6(H_2O)_3]^{2+}$,
(b) $[M_3(\mu_3\text{-}CCH_3)(\mu_3\text{-}O)(\mu\text{-}CH_3COO)_6(H_2O)_3]^+$, and
(c) $[W_3(\mu_3\text{-}O)(\mu\text{-}CH_3COO)_6(H_2O)_3]^{2+}$

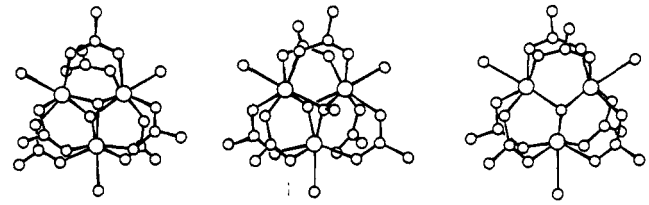

a b c

(1) Present address: Department of Chemistry, Faculty of Science, Saitama University, Shimo-okubo, Urawa 338, Japan.
(2) Cotton, F. A.; Wilkinson, G. *Advanced Inorganic Chemistry*, 5th ed.; Wiley: New York, 1988; p 824.
(3) Cotton, F. A. *Polyhedron* **1986**, *5*, 3–14 and references therein.
(4) Wang, B.; Sasaki, Y.; Nagasawa, A.; Ito, T. *J. Am. Chem. Soc.* **1986**, *108*, 6059–6060; *J. Coord. Chem.* **1988**, *18*, 45–61.
(5) Bino, A.; Cotton, F. A.; Dori, Z. *J. Am. Chem. Soc.* **1981**, *103*, 243–244.
(6) Bino, A.; Cotton, F. A.; Dori, Z.; Kolthammer, B. W. S. *J. Am. Chem. Soc.* **1981**, *103*, 5779–5784.
(7) Bino, A.; Cotton, F. A.; Dori, Z.; Falvello, L. R.; Reisner, G. M. *Inorg. Chem.* **1982**, *21*, 3750–3755.
(8) A Mo_3 complex with a CC_2H_5 cap is also known: Bino, A.; Gibson, D. *Inorg. Chim. Acta* **1982**, *65*, L37–L39.
(9) Cotton, F. A.; Dori, Z.; Kapon, M.; Marler, D. O.; Reisner, G. M.; Schwotzer, W.; Shaia, M. *Inorg. Chem.* **1985**, *24*, 4381–4384.
(10) Ardon, M.; Bino, A.; Cotton, F. A.; Dori, Z.; Kaftory, M.; Kolthammer, B. W. S.; Kapon, M.; Reisner, G. *Inorg. Chem.* **1981**, *20*, 4083–4090.
(11) Ardon, M.; Cotton, F. A.; Dori, Z.; Fang, A.; Kapon, M.; Reisner, G. M.; Shaia, M. *J. Am. Chem. Soc.* **1982**, *104*, 5394–5398.
(12) Bino, A.; Cotton, F. A.; Dori, Z.; Shaia-Gottlieb, M.; Kapon, M. *Inorg. Chem.* **1988**, *27*, 3592–3596.
(13) Wang, B. Ph.D. Thesis, Tohoku University, 1986.

0020-1669/91/1330-1575$02.50/0

derivative, $[Mo_3(\mu_3\text{-}CCH_3)(\mu_3\text{-}O)(\mu\text{-}CH_3COO)_6(py)_3]^+$. These two reactions would also provide the information on the influence of the leaving ligand. The CD_3OD substitution reaction (eq 4)

$$[W_3(\mu_3\text{-}O)(\mu\text{-}CH_3COO)_6(H_2O)_3]^{2+} + 3CD_3OD \rightarrow [W_3(\mu_3\text{-}O)(\mu\text{-}CH_3COO)_6(CD_3OD)_3]^{2+} + 3H_2O \quad (4)$$

of the single-capped complex $[W_3(\mu_3\text{-}O)(\mu\text{-}CH_3COO)_6(H_2O)_3]^{2+}$ has also been studied. This complex has both a different capping group and a different oxidation state from those of the previously studied[13] double-capped complex $[W_3(\mu_3\text{-}O)_2(\mu\text{-}CH_3COO)_6(H_2O)_3]^{2+}$ but is expected to provide useful comparative informations. In this paper, the CD_3OD substitution reactions (eqs 2 and 4) are reported first because of the similar experimental procedures for these reactions, and the pyridine-exchange reaction (eq 3) follows.

Experimental Section

Preparation of the Complexes. (1) $[Mo_3(\mu_3\text{-}CCH_3)(\mu_3\text{-}O)(\mu\text{-}CH_3COO)_6(py)_3](BF_4)\cdot 0.5py$. The tris(aqua) complex $[Mo_3(\mu_3\text{-}CCH_3)(\mu_3\text{-}O)(\mu\text{-}CH_3COO)_6(H_2O)_3]BF_4$[6] was dissolved in a small amount of pyridine, and the solution was kept at 40 °C for 12 h and then at room temperature for 20 days. On addition of diethyl ether, the tris(pyridine) complex was precipitated, which was filtered and washed with diethyl ether and dried. Anal. Calcd: C, 36.07; H, 3.70; N, 4.67. Found: C, 35.67; H, 3.69; N, 5.23. Electronic absorption maxima in pyridine: λ_{max} = 340 nm (ϵ/M^{-1} cm^{-1} = 2586), 403 nm (3508). IR data (KBr disk) (cm^{-1}): 580 m, 760 w, 1020 w, 1060 br, 1220 w, 1360 w, 1450 s, 1490 w, 1560 s, 1610 w, 3420 br. NMR data: ^{1}H NMR in CD_3NO_2 vs TMS at δ 0, 2.58 (s, 3 H, μ_3-CCH_3), 2.13 (s, 9 H, CH_3COO), 2.23 (s, 9 H, CH_3COO), 7.71 (t, 6 H, Mo–py 3,5-H), 8.16 (t, 3 H, Mo–py 4-H), 9.22 (d, 6 H, Mo–py 2,6-H), 7.42 (t, 1 H, free py 3,5-H), 7.83 (t, 0.5 H, free py 4-H), 8.58 (d, 1 H, free py 2,6-H); $^{13}C\{^1H\}$ in CD_3NO_2 vs TMS at δ 0, 23.7 (CH_3COO), 23.9 (CH_3COO), 32.4 (μ_3-CCH_3), 184.38 (CH_3COO), 184.44 (CH_3COO), 296.8 (μ_3-CCH_3), 125.6 (coordinated py C-3), 141.5 (coordinated py C-4), 151.7 (coordinated py C-2), 124 (free py C-3), 130 (free py C-4), 149 (free py C-2); ^{95}Mo NMR in CH_3CN vs MoO_4^{2-} at δ 0, 1447. The complex is soluble in CH_3CN, CH_3NO_2, pyridine, and acetone and slightly soluble in methanol. It is insoluble in water, ethanol, and diethyl ether.

(2) Other Complexes. $[Mo_3(\mu_3\text{-}CCH_3)(\mu_3\text{-}O)(\mu\text{-}CH_3COO)_6(H_2O)_3]^{+}$[6] and $[W_3(\mu_3\text{-}O)(\mu\text{-}CH_3COO)_6(H_2O)_3]^{2+}$[11] were prepared by the reported methods of Cotton and co-workers. The complex ions were eluted with HCl solution from a Dowex 50W-X2 cation-exchange column and isolated as the chloride and trifluoromethanesulfonate salts, respectively, as follows. $[Mo_3(\mu_3\text{-}CCH_3)(\mu_3\text{-}O)(\mu\text{-}CH_3COO)_6(H_2O)_3]Cl$ was obtained by slow evaporation of the eluate, while $[W_3(\mu_3\text{-}O)(\mu\text{-}CH_3COO)_6(H_2O)_3](CF_3SO_3)_2$ was obtained by addition of CF_3SO_3Na (*Caution*! The perchlorate salt of the W complex is explosive in the dried solid state, and this preparation should be avoided when any alternative salt can be substituted.) NMR data for $[Mo_3(\mu_3\text{-}CCH_3)(\mu_3\text{-}O)(\mu\text{-}CH_3COO)_6(H_2O)_3]^+$: ^{1}H NMR in D_2O/DCl vs DSS ($(CH_3)_3Si(CH_2)_3SO_3Na$) at δ 0, 2.38 (s, 3 H, μ_3-CCH_3), 2.19 (s, 9 H, CH_3COO), 2.12 (s, 9 H, CH_3COO); $^{13}C\{^1H\}$ in D_2O/DCl vs DSS at δ 0, 25.1 (CH_3COO), 25.2 (CH_3COO), 33.5 (CCH_3), 186.3 (CH_3COO), 186.9 (CH_3COO), 300.0 (CCH_3); ^{95}Mo NMR in 6 M HCl vs MoO_4^{2-} at δ 0, 1464. NMR data for $[W_3(\mu_3\text{-}O)(\mu\text{-}CH_3COO)_6(H_2O)_3]^{2+}$: ^{1}H NMR in $D_2O/DClO_4$ vs DSS at δ 0, 2.57 (s, 9 H, CH_3COO), 2.53 (s, 9 H, CH_3COO); $^{13}C\{^1H\}$ in $D_2O/DClO_4$ vs DSS at δ 0, 24.6 (CH_3COO), 25.6 (CH_3COO), 189.6 (CH_3COO), 202.9 (CH_3COO); ^{183}W NMR in 0.2 M HCl vs WO_4^{2-} at δ 0, 4708.

(3) Other Materials. CD_3OD (99% deuterated) and C_5D_5N (100%) from Aldrich and D_2O (99.75%) from Merck were used without further purification. CD_3NO_2 (99%) from Merck and CH_3NO_2 from Wako were dried on 4A molecular sieves and distilled. CH_3CN was distilled over P_4O_{10} and CaH_2, successively.

Measurements. ^{1}H and ^{13}C NMR spectra were measured on a JEOL GSX-270 FT-NMR spectrometer at 270 and 67.9 MHz, respectively. A Bruker AM-600 (600 MHz) FT-NMR spectrometer was also used for the measurement of a ^{1}H NMR spectrum. The variable-temperature kinetic studies were carried out by using the JEOL spectrometer with a variable-temperature controller. Temperature was calibrated within an accuracy of ±0.2 °C by using the chemical shift difference between the methyl and hydroxy signals of methanol. Ultraviolet and visible absorption spectra were measured with a Hitachi 340 spectrophotometer. Infrared absorption spectra were measured with a JASCO IR-810 spectrophotometer on KBr pellets at room temperature. Cyclic voltammograms were obtained in CH_3CN and CH_3NO_2 solutions by using a Yanaco P-1100 polarographic analyzer with a glassy-carbon working electrode, Pt counter electrode, and $Ag/AgClO_4$ (0.1 M) reference electrode. Potentials were reported with reference to the ferrocene/ferrocenium ($Fe(cp)_2/Fe(cp)_2^+$) potential at 0 V.

Kinetic Procedures. A small amount of the complex was dissolved in the cooled solvent (−80 to −90 °C), and the sample solution was quickly placed in the NMR cell compartment, which was kept at the desired temperature. In the case of the pyridine-exchange reaction, a certain amount of pyridine-d_5 was added to the solvent CD_3NO_2 in advance. The reactions were followed at a certain interval, and the relative integrated intensity of relevant signals was obtained to evaluate rate constants.

Results and Discussion

Characterization of the New Complex $[Mo_3(\mu_3\text{-}CCH_3)(\mu_3\text{-}O)(\mu\text{-}CH_3COO)_6(py)_3]^+$. ^{1}H and ^{13}C NMR spectra clearly support that pyridines coordinate at all three terminal positions and that the μ_3-CCH_3-μ_3-oxo structure is retained. All the ^{1}H NMR and ^{13}C NMR chemical shifts of the acetates and the capping CCH_3 group are very similar to the corresponding shifts of the aqua complex. The pyridine complex is reversibly oxidized at $E_{1/2}$ = +0.43 V vs $Fe(cp)_2/Fe(cp)_2^+$ in CH_3NO_2, which is considerably less positive than the $E_{1/2}$ value (+0.52 V) of the aqua complex in the same solvent. The cluster core would have higher electron density by the coordination of more basic pyridine and is oxidized more easily. The $E_{1/2}$ value of the pyridine complex in CH_3CN is +0.41 V.[14] The absorption spectrum of the pyridine complex is similar in pattern to that of the aqua complex at >300 nm, but the visible absorption maximum shifts considerably to lower energy (from 379 to 403 nm) with a small increase in intensity.[15]

Change in the ^{1}H NMR Spectra of the Two Tris(aqua) Complexes in CD_3OD. The acetate methyl signals of the ^{1}H NMR spectra of the two complexes $[Mo_3(\mu_3\text{-}CCH_3)(\mu_3\text{-}O)(\mu\text{-}CH_3COO)_6(H_2O)_3]^+$ and $[W_3(\mu_3\text{-}O)(\mu\text{-}CH_3COO)_6(H_2O)_3]^{2+}$ change their patterns with time in CD_3OD. The changes are due to the successive substitution of CD_3OD for the three aqua ligands.

$$M_3L(H_2O)_3 \xrightarrow{k_1} M_3L(H_2O)_2(CD_3OD) \xrightarrow{k_2} M_3L(H_2O)(CD_3OD)_2 \xrightarrow{k_3} M_3L(CD_3OD)_3 \quad (5)$$

Here M_3L represents either the $Mo_3(\mu_3\text{-}CCH_3)(\mu_3\text{-}O)(\mu\text{-}CH_3COO)_6$ or the $W_3(\mu_3\text{-}O)(\mu\text{-}CH_3COO)_6$ moiety. Figure 1 shows the change with time in the ^{1}H NMR spectrum of $[W_3(\mu_3\text{-}O)(\mu\text{-}CH_3COO)_6(H_2O)_3]^{2+}$ in CD_3OD. Immediately after the dissolution, two methyl signals with identical integrated intensities were observed, which represent two types of the acetate ligands on the same side as and the opposite side to the μ_3-oxo ligand with respect to the W_3 plane. Each of the two methyl signals shows an almost identical change; two signals appear at the lower field side at the expense of the original higher field signals. For each methyl group, we expect six different chemical environments during the successive substitution of CD_3OD for the three aqua ligands. Although further splitting was not clearly observed in 270-MHz NMR spectra (Figure 1), a 600-MHz ^{1}H NMR spectrum taken after ca. 30 min at 30 °C (Figure 2) clearly shows all the 12 signals expected. All the signals in Figure 2 are assigned as indicated in Chart II. In this chart, signals A, B, and C represent the acetate ligands in $(H_2O)W(\mu\text{-}CH_3COO)W(H_2O)$, $(CD_3OD)W(\mu\text{-}CH_3COO)W(H_2O)$, and $(CD_3OD)W(\mu\text{-}CH_3COO)W(CD_3OD)$ moieties, respectively.

Figure 3 shows similar spectral change for $[Mo_3(\mu_3\text{-}CCH_3)(\mu_3\text{-}O)(\mu\text{-}CH_3COO)_6(H_2O)_3]^+$. Splitting of the signal of the capping CCH_3 is small, and complete separation was not observed.

Kinetic Analysis of the Substitution Reactions in CD_3OD. Since the splitting of each of the signals A, B, and C was not clear with a 270-MHz NMR spectrum, the overall intensity change of each signal was analyzed for the kinetic treatment. Figure 4 shows

(14) The $E_{1/2}$ value of the aqua complex in CH_3CN was +0.45 V, which probably represents the $(CH_3CN)_3$ species rather than the tris(aqua) complex.

(15) Our ϵ value of the absorption maximum at 379 nm of the aqua complex is 3378 M^{-1} cm^{-1}, which is more than 10 times bigger than the reported value (298 M^{-1} cm^{-1}).[6] The latter value could be in error by a factor of 10.

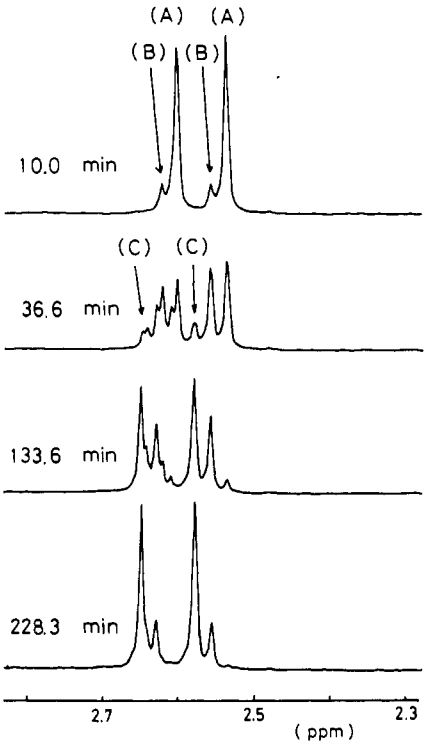

Figure 1. Time dependence of the ^{1}H NMR spectrum of $[W_3(\mu_3\text{-}O)(\mu\text{-}CH_3COO)_6(H_2O)_3](CF_3SO_3)_2$ in CD_3OD at 30 °C.

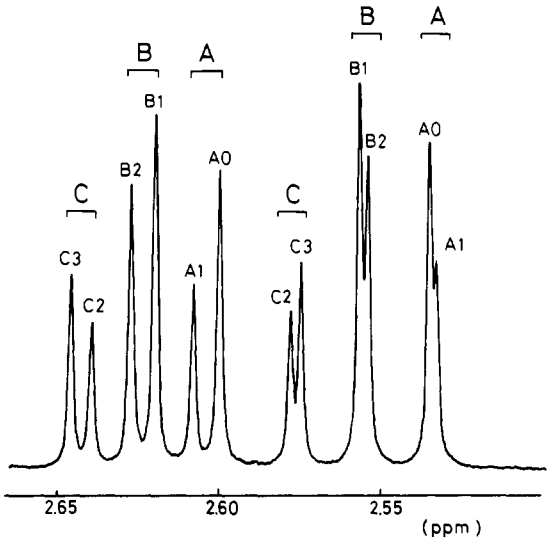

Figure 2. 600-MHz ^{1}H NMR spectrum of $[W_3(\mu_3\text{-}O)(\mu\text{-}CH_3COO)_6(H_2O)_3](CF_3SO_3)_2$ in CD_3OD at 30 °C measured ca. 30 min after the dissolution.

the time dependence of the relative integrated intensity (signal area) of each of the three signals, A, B, and C, for the W_3 complex. Each signal area, which is expressed as a, b, or c, respectively, represents a composite of the two species. For example, the signal area a represents the entire signal of the species $W_3L(H_2O)_3$ and one-third of the signal of $W_3L(H_2O)_2(CD_3OD)$. The overall signal area of the species, $W_3L(H_2O)_{3-n}(CD_3OD)_n$ is defined as $S(n)$. Then the $S(0)$ is expressed as in eq 6. If $S(3)$ is neglected for

$$S(0) = a - b/2 + c - S(3) \quad (6)$$

the evaluation of the rate constant of the first step, then k_1 is expressed as in eq 7. The plot of the left-hand side of eq 7 against

$$\ln\{(a - b/2 + c)/(a + b + c)\} = -k_1 t \quad (7)$$

t gave a straight line,[16] from the slope of which k_1 was estimated.

(16) The plot deviates from the straight line after approximately 1 half-life, which may be due to the contribution of $S(3)$.

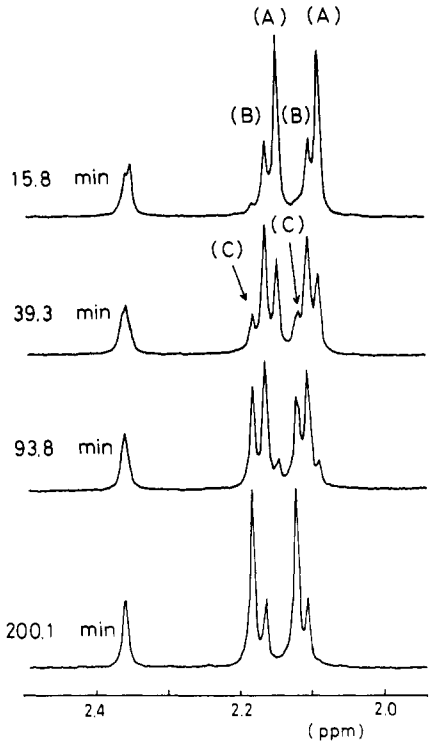

Figure 3. Time dependence of the ^{1}H NMR spectrum of $[Mo_3(\mu_3\text{-}CCH_3)(\mu_3\text{-}O)(\mu\text{-}CH_3COO)_6(H_2O)_3]Cl$ in CD_3OD at −15 °C.

Chart II. Assignment of the ^{1}H NMR Signals of the Species $M_3L(CD_3OD)_n(H_2O)_{3-n}$ (M_3L = $Mo_3(\mu_3\text{-}CCH_3)(\mu_3\text{-}O)(\mu\text{-}CH_3COO)_6$ or $W_3(\mu_3\text{-}O)(\mu\text{-}CH_3COO)_6$)

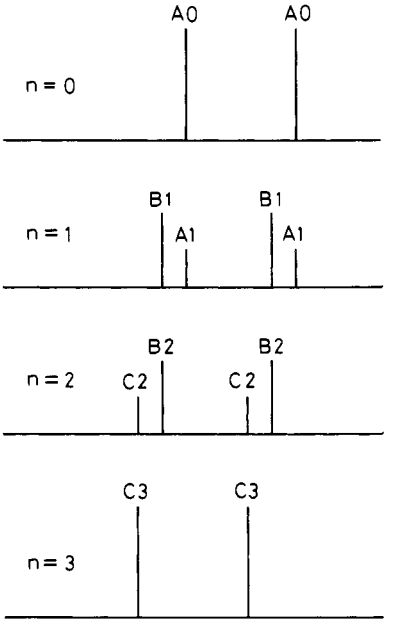

Table I. First-Order Rate Constants per W for the Stepwise Substitution of CD_3OD for the Coordinated Water Ligands in $[W_3(\mu_3\text{-}O)(\mu\text{-}CH_3COO)_6(H_2O)_3]^{2+}$ in CD_3OD

temp/°C	$k_1/10^{-5}$ s^{-1} [a]	$k_2/10^{-5}$ s^{-1}	$k_3/10^{-5}$ s^{-1}
9.5	0.5 ± 0.1, 0.5 ± 0.1		
19.5	2.6 ± 0.3, 2.6 ± 0.5		
24.5	5.4 ± 0.6, 5.6 ± 0.6		
29.6	14.4 ± 2.5, 12.0 ± 0.3	ca. 18[b]	ca. 14[b]

$\Delta H^{\ddagger}_1 = 113 \pm 3$ kJ mol^{-1}
$\Delta S^{\ddagger}_1 = +56 \pm 9$ J K^{-1} mol^{-1}

[a] Two values were obtained from the methyl signals at higher and lower magnetic field, respectively. [b] Obtained from the methyl signal at higher field.

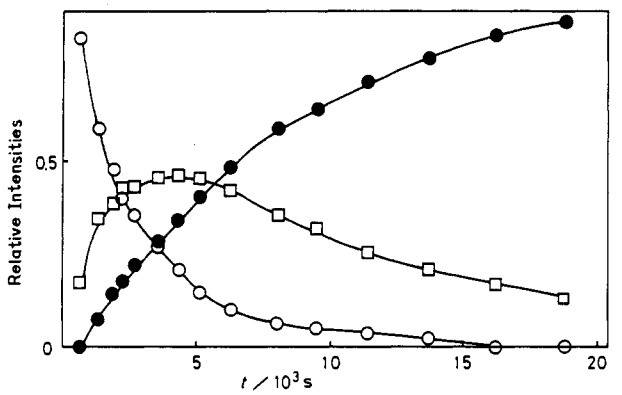

Figure 4. Time dependence of the relative integrated intensities of signals A, B, and C (Figure 1) of the ^{1}H NMR spectrum of $[W_3(\mu_3\text{-}O)(\mu\text{-}CH_3COO)_6(H_2O)_3](CF_3SO_3)_2$ in CD_3OD at 30 °C: (○) peak A; (□) peak B; (●) peak C.

Table II. First-Order Rate Constants per Mo for the Stepwise Substitution of CD_3OD for the Coordinated Water Ligands in $[Mo_3(\mu\text{-}CCH_3)(\mu_3\text{-}O)(\mu\text{-}CH_3COO)_6(H_2O)_3]^+$ in CD_3OD

temp/°C	$k_1/10^{-5}$ s^{-1} [a]	$k_2/10^{-5}$ s^{-1}	$k_3/10^{-5}$ s^{-1}
−30.2	1.7 ± 0.1		
−25.2	4.3 ± 0.3		
−22.5	9.4 ± 1.5		
−15.3	24.9 ± 5.9	ca. 21	ca. 14

$\Delta H^*_1 = 93 \pm 11$ kJ mol^{-1}
$\Delta S^*_1 = +49 \pm 47$ J K^{-1} mol^{-1}

[a] Obtained from the methyl signals at higher field.

The k_1 values obtained from the two different methyl signals are in reasonable agreement. The rate constants k_2 and k_3 were roughly estimated by the computer simulation of the time dependence of each signal given in Figure 4. The k_1, k_2, and k_3 values are summarized in Table I. Activation parameters, ΔH^* and ΔS^*, were obtained from the temperature dependence of k (Table I). The rate constants for the reaction of $[Mo_3(\mu_3\text{-}CCH_3)(\mu_3\text{-}O)(\mu\text{-}CH_3COO)_6(H_2O)_3]^+$ were similarly evaluated. Signal A of the methyl peak of the lower field was overlapped with signal C of the higher field peak, and the k_1 value was obtained less accurately. Thus the rate constants were obtained from the higher field peak only. Rate constants and activation parameters were summarized in Table II.

Rate constants of the second and the third steps may be considered to be similar to that of the first step for both of the complexes. Thus the substitution takes place almost independently at each site of the trinuclear complexes. Ligand-substitution reactions of another type of the trinuclear molybdenum(IV) complex $[Mo_3O_4(H_2O)_9]^{4+}$ have been reported, in that the three metal centers behave independently.[17,18]

Pyridine-Exchange Reactions. On addition of py-d_5 to the CD_3NO_2 solution of $[Mo_3(\mu_3\text{-}CCH_3)(\mu_3\text{-}O)(\mu\text{-}CH_3COO)_6(py)_3]^+$, signal intensities of the coordinated pyridine decrease with simultaneous increase in those of the free pyridine. The acetate methyl signals are not affected at all during the change. An example of the spectral change is shown in Figure 5. The change should be due to the substitution of py-d_5 for the coordinated py (eq 3). If the change were due to the solvolysis rather than the pyridine exchange, a shift or splitting of the methyl signals would have been observed as in the case of the substitution reactions of CD_3OD (vide supra). The rate constants for the exchange reaction were evaluated from the intensity change of the 2,6-position proton signal of pyridine by the use of the following McKay type equation.[19]

$$\ln \{(I_t - I_\infty)/(I_0 - I_\infty)\} = -\{(3m + n)/(3mn)\}Rt + \text{const} \quad (8)$$

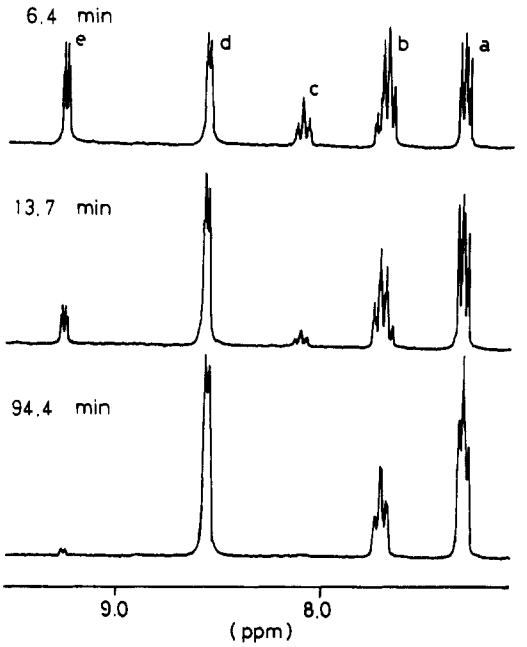

Figure 5. Time dependence of the ^{1}H NMR spectrum of $[Mo_3(\mu_3\text{-}CCH_3)(\mu_3\text{-}O)(\mu\text{-}CH_3COO)_6(py)_3]BF_4$ in CD_3NO_2 containing py-d_5 at 30 °C: signals a and d, free pyridine; signals c and e, coordinated pyridine; signal b, overlap of free and coordinated pyridine.

Table III. Rate Constants for the Pyridine-Exchange Reaction of $[Mo_3(\mu_3\text{-}CCH_3)(\mu_3\text{-}O)(\mu\text{-}CH_3COO)_6(py)_3]^+$ in CD_3NO_2 with Pyridine-d_5

temp/°C	[complex]/M	[py-d_5]/M	$k_0/10^{-5}$ s^{-1}
−0.3	0.023	0.69	2.3
9.8	0.023	0.52	12.1
9.8	0.022	1.29	14.0
9.8	0.020	1.84	14.1
20.6	0.022	1.29	81.0
20.8	0.023	0.52	79.5
20.8	0.020	1.84	85.8
20.8	0.050	2.61	96.8
34.6	0.023	0.52	671.6
34.6	0.022	1.29	678.6
34.6	0.023	1.99	743.8

$\Delta H^*_1 = 112 \pm 1$ kJ mol^{-1}
$\Delta S^*_1 = +77 \pm 5$ J K^{-1} mol^{-1}

Here m and n are the initial concentrations of the complex and py-d_5, respectively. I is equal to $p/(p + q)$ (p and q are the relative integrated intensities of ^{1}H NMR signals of the coordinated and the free pyridine, respectively). The plot of the left-hand side of eq 8 against t gave a good straight line, from the slope of which R ($=k_0/m$) was evaluated. Results were summarized in Table III. The rate constant is practically independent of the initial concentration of py-d_5.

Mechanism of the Substitution Reactions. Stereochemical consideration alone is in favor of the dissociative mechanism. Since the coordinated acetate oxygens bend toward the substitution site (O(acetate)–M–O(H_2O) = ca. 75°), associative attack of the incoming ligand in this compound is far more difficult as compared with attack in normal octahedral complexes. The following experimental facts support the assignment of I_d or even D mechanism for the present substitution reactions. (i) Independence of the rate constant on [pyridine-d_5] suggests that the D mechanism operates at least for the pyridine-exchange reaction. (ii) Significant dependence of the rate constant on the nature of the leaving ligands, H_2O or pyridine, indicates the importance of the bond break rather than the bond formation. (iii) Large ΔH^* and positive ΔS^* values point to the dissociative mechanism. The

(17) Ooi, B.-L.; Sykes, A. G. *Inorg. Chem.* **1988**, *27*, 310–315.
(18) Kathirgamanathan, P.; Soares, A. B.; Richens, D. T.; Sykes, A. G. *Inorg. Chem.* **1985**, *24*, 2950–2954.
(19) McKay, H. A. C. *Nature (London)* **1938**, *142*, 997–998.

dissociative mechanism should be related to the "trans effect" of the μ_3-ligand. The Mo–O(H_2O) distance (2.159–2.194 Å)[6,7] of the μ_3-CCH_3 complex is larger than that (2.083–2.129 Å)[20,21] of the bis(μ_3-oxo) complex, suggesting the importance of the bond break.

Effect of the Capping Ligand and the Oxidation State. The first-order rate constants of the substitution reactions of CD_3OD for the terminal aqua ligands on $[Mo_3(\mu_3\text{-}O)_2(\mu\text{-}CH_3COO)_6(H_2O)_3]^{2+}$ and $[W_3(\mu_3\text{-}O)_2(\mu\text{-}CH_3COO)_6(H_2O)_3]^{2+}$ are 1.1×10^{-5} and $<5 \times 10^{-7}$ s^{-1}, respectively, at 44.8 °C.[13] The rate constant (1.2 s^{-1}) of the Mo_3–μ_3-CCH_3 complex at 44.8 °C as calculated from the activation parameters is larger by ca. 10^5 times than the corresponding rate constant for the bis(μ_3-oxo) complex. Since the formal oxidation states are the same (IV,IV,IV) and the Mo–Mo distances are similar between two complexes,[5,6,20,21] different capping ligands must be almost entirely responsible for the 10^5 times difference in the rate constants. Thus the μ_3-CCH_3 ligand has a significantly larger trans effect as compared with that of the oxide cap.[22]

It would be appropriate to discuss here further on the trans effect of the oxide cap. Richens et al. showed in the study of the water exchange of a different type of trinuclear molybdenum(IV) complex ion, $[Mo_3(\mu_3\text{-}O)(\mu\text{-}O)_3(H_2O)_9]^{4+}$, that the water ligands trans to the μ_2-oxo is ca. 10^5 times more labile than the one trans to the μ_3-oxide.[23] It is not clear in this case if the μ_3-oxide has any trans effect.[24] In the reactions of these molybdenum complexes, evaluation of the trans effect of the oxide cap is difficult, since the reference data on the "intrinsic substitution rate of molybdenum(IV)" (represented by the lability of postulated $[Mo(H_2O)_6]^{4+}$) either is not available or is not easy to estimate. We have shown the existence of the trans effect of the μ_3-oxide for the CD_3OD substitution for the coordinated water ligands in $[M^{III}_3(\mu_3\text{-}O)(\mu\text{-}CH_3COO)_6(H_2O)_3]^{+}$ (M_3 = Ru_3, Rh_3, or Ru_2Rh), where the substitutions at tervalent ruthenium and rhodium centers are 10^2–10^4 times faster than the water-exchange reactions of the uninuclear complexes of these metal ions.[25,26]

The rate constant of the W_3–mono(μ_3-oxo) complex (estimated to be 1.2×10^{-3} s^{-1} at 44.8 °C) is at least 2×10^3 times larger than the corresponding value of the W_3–bis(μ_3-oxo) complex. Interpretation of the result is not as simple as in the above case, since the difference in both the number of the oxide caps and the formal oxidation state have to be taken into account. If the trans effect of the capping group is important, we would expect a decrease in the rate constant for the mono(μ_3-oxo) complex. Thus the different oxidation state is more likely to be the controlling factor in this case. This is consistent with the general trend that the decrease in the oxidation state causes the increase in the substitution rate if the electronic configurations are similar. It is difficult at the present stage to discuss the effect of electronic state (more specifically, d-electron number) of the cluster core on the ligand substitution. The W–W bond may play some role, since the W–W distance of the mono(μ_3-oxo) complex[11,12] is shorter and therefore the W–W bond is stronger than in the bis(μ_3-oxo) complex.[27,28]

Acknowledgment. This work was supported by a Grant-in-Aid for Scientific Research (No. 02245106) on the Priority Area of "Molecular Approaches to Non-equilibrium Processes in Solutions" and a Grant-in-Aid for Scientific Research (No. 01430009) from the Ministry of Education, Science, and Culture, Japan.

(20) Ardon, M.; Bino, A.; Cotton, F. A.; Dori, Z.; Kaftory, M.; Reisner, G. M. *Inorg. Chem.* **1982**, *21*, 1912–1917.
(21) Cotton, F. A.; Dori, Z.; Marler, D. O.; Schwotzer, W. *Inorg. Chem.* **1983**, *22*, 3104–3106.
(22) The ^{13}C and ^{95}Mo chemical shifts of $[Mo_3(\mu_3\text{-}CCH_3)(\mu_3\text{-}O)(\mu\text{-}CH_3COO)_6(H_2O)_3]^{+}$ (see Experimental Section) indicate a significant deshielding at CCH_3 and a slightly lower oxidation state of Mo than that of the $(\mu_3\text{-}O)_2$ complex (see discussions in: Nagasawa, A.; Sasaki, Y.; Wang, B.; Ikari, S.; Ito, T. *Chem. Lett.* **1987**, 1271–1274), which may be due to the strong electron releasing effect of CCH_3^{3-}. It follows then that the increase in the substitution rate would be at least partly explained by the higher electron density of the Mo_3 moiety as discussed for the W_3 mono(oxo)-capped complex.
(23) Richens, D. T.; Helm, L.; Pittet, P.-A.; Merbach, A. E.; Nicolo, F.; Chapius, G. *Inorg. Chem.* **1989**, *28*, 1394–1402.
(24) It should be noted that the water exchange occurs exclusively via a $[H^+]^{-1}$-dependent pathway, i.e., a conjugate base mechanism.[23]
(25) Sasaki, Y.; Tokiwa, A.; Ito, T. *J. Am. Chem. Soc.* **1987**, *109*, 6341–6347.
(26) Sasaki, Y.; Tokiwa, A.; Nagasawa, A.; Ito, T. Manuscript in preparation.
(27) Bino, A.; Cotton, F. A.; Dori, Z.; Koch, S.; Kuppers, H.; Millar, M.; Sektowski, J. C. *Inorg. Chem.* **1978**, *17*, 3245–3253.
(28) Bino, A.; Hesse, K.-F.; Kuppers, H. *Acta Crystallogr., Sect. B: Struct. Crystallogr. Cryst. Chem.* **1980**, *B36*, 723–725.